Investigation of the influence of viscoelastic behaviour on the agitation of non-Newtonian fluid flow

T. Reviol, S. Kluck, F. Genuit, V. Reim, M. Böhle

Chemical Engineering Science

www.elsevier.com/locate/ces

PII: S0009-2509(16)30283-4
DOI: http://dx.doi.org/10.1016/j.ces.2016.05.035
Reference: CES12974

To appear in: *Chemical Engineering Science*

Received date: 7 December 2015
Revised date: 15 December 2015
Accepted date: 24 May 2016

Cite this article as: T. Reviol, S. Kluck, F. Genuit, V. Reim and M. Böhle, Investigation of the influence of viscoelastic behaviour on the agitation of non Newtonian fluid flow, *Chemical Engineering Science* http://dx.doi.org/10.1016/j.ces.2016.05.035

Investigation of the influence of viscoelastic behaviour on the agitation of non-Newtonian fluid flow

T. Reviol[a,*], S. Kluck[a], F. Genuit[a,1], V. Reim[a], M. Böhle[a]

[a] *Technical University of Kaiserslautern, Department of Mechanical and Process Engineering, Institute of Fluid Mechanics and Fluid Machinery, Gottlieb-Daimler Straße, Building 44, 67663 Kaiserslautern, Germany*

Abstract

The design process of mixers agitating non-Newtonian fluid flow is usually performed with several well-known correlation methods. These methods has been the issue of many studies of the last few decades, so they are well discovered and often extended. But these studies also disclose the dependency of the correlation methods on the rheology of the fluid flow. Due to the good applicability the discovered dependencies were often neglected. In this paper the existing methods will be investigated experimentally for agitating viscoelastic as well as viscoinelastic fluid flow to determine the influence of viscoelasticity on the power consumption of agitating non-Newtonian fluid flow.

Keywords: design method, mixing, non-Newtonian Flow, Power consumption, viscoelastic

*Corresponding author

Email addresses: reviol@mv.uni-kl.de (T. Reviol), stefan.kluck@mv.uni-kl.de (S. Kluck), genuit@iag.uni-stuttgart.de (F. Genuit), vreim@rhrk.uni-kl.de (V. Reim), martin.boehle@mv.uni-kl.de (M. Böhle)

[1]Present address: University of Stuttgart, Faculty 6: Aerospace Engineering and Geodesy, Institute of Aerodynamics and Gas Dynamics, Pfaffenwaldring 21, 70569 Stuttgart, Germany

1. Introduction

The estimation of the power consumption for mixing processes of non-Newtonian fluid flow is usually performed by several correlation methods. These methods are based on the power consumption of mixing Newtonian fluid flow.

The correlation process is necessary because the viscosity of the non-Newtonian fluid depends on the local shear rate. Since the shear rate is typically unknown before the mixing process is developed, the design process can't be performed without the correlation with Newtonian power characteristics.

The common methods to design mixing processes are investigated by Metzner and Otto <1> and by Rieger and Novak <2; 3; 4>. Both methods were often improved. Henzler et. al. proposed a concept based on the power of the mixer instead on the shaft speed, as introduced by Metzner and Otto <5>. A very similar concept was chosen by Wassmer et. al. <6>. Reviol recommended a concept based on the power, which is developed using an analytic formulation of the mixing process. The concept can be transformed to the concept by Wassmer et. al. and was confirmed by experimental investigations <7; 8; 9>. A summary of the established methods can be found in <10> and <11>.

Although the concepts by Metzner and Otto and by Rieger and Novak are state of the art, these concepts were often criticized. Especially the dependency of Metzner's and Otto's concept on the mixed fluid was emphasized <12; 13; 14>, but also the missing of the dimensional accuracy <15>, which possibly leads to wrong power calculation <16>. The concept by Rieger and

Novak was also criticized, but has been confirmed for creeping flow by <17> and <18>. In spite of all these disadvantages, both concepts are usually applied due to their simplicity <19>.

A few years ago, Höcker et. al. identified the correlation factor by Metzner and Otto beeing a function of the fluid flow, too. This was the first time, the concept by Metzner and Otto was related to the viscoelasticity of a fluid <13>. Reviol et. al. also discovered the dependency of this concept on the fluid as well as on their own concept <7; 8; 9>. Neither Höcker et. al. nor Reviol et. al. performed investigations in purely viscous and viscoelastic fluid flow. So, a comparison is still missing.

In this paper, the comparison of the effects of various non-Newtonian fluid flow on the mixing process is investigated. The experiments are performed for fluids, which are purely viscous and for fluids with viscoelastic behaviour.

2. Fundamentals of Rheology

A substantial problem in analysing literature that handles the power consumption of agitating non-Newtonian fluid flow and its dependencies is the inadequate documen-tation of the physical parameters of the used fluids for the mixing process. Model fluids can be prepared and analysed using various methods. This causes differences in interpreting the performed measurement values. Especially the differences in measuring physical properties of the fluid cause misunderstandings.

Hence, all in this study used methods to characterize fluid properties will be clearly described.

2.1. Purely viscous fluid flow

If the state of stress is totally characterized by the shear viscosity μ, the fluid will be purely viscous. A more ideal case is given for a constant viscosity and is described by Newton's law, see equation 1. Herein, τ is the shear stress and $\dot{\gamma}$ the shear rate.

$$\tau = \mu \cdot \dot{\gamma} \tag{1}$$

In real processes, the shear viscosity is usually variable. In the process industry, especially the dependency on the deformation state is highly important. The deformation state can cause either pseudoplastic or dilatant fluid behaviour. In the present study, all discussed investigations were carried out with pseudoplastic fluid behaviour.

The mathematical formulation of non-Newtonian viscous fluid flow is typically done by applying several empirical laws. These laws approximate the shear stress or the viscosity as a function of the shear rate. A very common law is the power-law by Ostwald and DeWaele according to equation 2. Herein k is called consistency and m flow index.

$$\tau = \mu \cdot \dot{\gamma}^m \tag{2}$$

For a better approximation, equation 2 can be extended by the summand a, see equation 3. The dimension of the Parameter a is the same as for the shear stress τ.

$$\tau = \mu \cdot \dot{\gamma}^m - a \tag{3}$$

By the application of a power law, the range of very low and very high shear rates will be neglected. These ranges are each identified with a constant shear viscosity, which can't be represented by a power law. Many technical processes are between these ranges, so the application of a power law for the technical fluids sector is acceptable due to the insignificance of these two ranges for the process <20>. In the present paper, the purely viscous fluid properties will be described by the parameters according to equation 3.

2.2. Viscoelastic fluid flow

If the state of stress depends on viscous and elastic properties, the fluid will be characterized being viscoelastic. For a deformation with sufficing small amplitudes, the fluid flow can be described with models for linearly viscoelastic (LVE) fluids.

One model to describe LVE-fluids was introduced by Maxwell, see figure 1. The model consists of a dashpot and a spring element. The dashpot element characterizes the shear viscosity μ while the spring element describes the elastic behaviour by the rigidity modulus G_0.

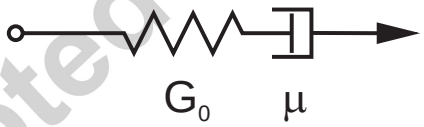

Figure 1: Maxwell model

Hence, a deformation that causes the shear rate $\dot{\gamma}$ can be separated in its viscous part $\dot{\gamma}_{\text{visc}}$ and its elastic part $\dot{\gamma}_{\text{elast}}$. The sum of both parts, together with the laws by Newton and Hooke will lead to the differential equation 4.

$$\dot{\gamma} = \dot{\gamma}_{\text{visc}} + \dot{\gamma}_{\text{elast}} = \frac{\tau}{\mu} + \frac{\dot{\tau}}{G_0} \tag{4}$$

Deforming a fluid according to equation 4 by a sudden impulse and observing this fluid for an adequate time interval, it will be clear that the normalized shear stress is fading, as can be seen in figure 2. Typically the shear stress is standardized with the shear strain γ_0 of the sudden impulse. The fading starts from the rigidity modulus G_0 and can be represented by the substance-related relaxation function $G(t)$. The time to describe the relaxation can be characterized by the relaxation time λ.

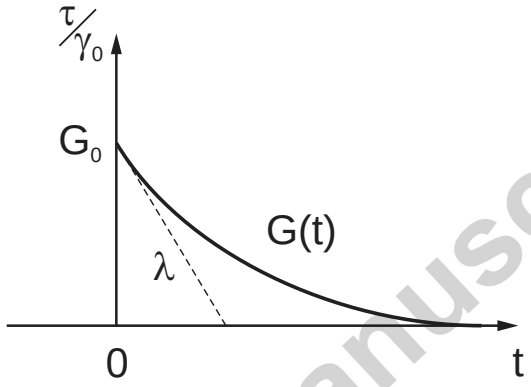

Figure 2: relaxation function

Equation 5 gives the well-known relation between shear viscosity and stress relaxation.

$$\mu = \lambda \cdot G_0 \tag{5}$$

Considering equation 5 the differential equation 4 can be written as:

$$\tau + \lambda \cdot \dot{\tau}(t) = \mu \cdot \dot{\gamma}(t) \tag{6}$$

With equation 6, the description of the actual state of stress of a LVE-fluid is possible. For the ideal case of a purely viscous fluid, the relaxation time

will be $\lambda = 0$ and equation 6 transforms into equation 1. For this reason, the viscoelastic character of a fluid can be specified by the relaxation time λ. This thesis is provided by experimental investigations of water, which is almost purely viscous. For water a relaxation time of approximately $\lambda = 1 \cdot 10^{-12}\ s$ can be measured. In contrast, melts of macromolecules show relaxation times of up to $\lambda = 1 \cdot 10^{2}\ s$ <21>.

Hence, in the present investigation the relaxation time of the Maxwell model is adopted to characterize the viscoelastic behaviour of the considered fluids.

2.3. Generalized Maxwell model

The Application of the Maxwell model on real fluids is often inappropriate. For macromolecule melts, Mezger proposes the following description: A single Maxwell model will represent a fraction with the same mole weight in a good accordance. But real molecular melts will consist in different molecular weights <22>. Therefore an arbitrary number of single Maxwell elements will be connected in parallel order. Figure 3 illustrates a generalized Maxwell model in an exemplary arrangement.

The Application of a generalized Maxwell model allows the estimation of the relaxation function with equation 7 <20; 23>. Herein, the parameters G_j and λ_j represent the discrete values of the relaxation function, respectively the relaxation time of a certain single Maxwell element.

$$G(t) = \sum_{j=1}^{z} G_\mathrm{j} \cdot \exp\left(-t/\lambda_\mathrm{j}\right) \tag{7}$$

To determine the mean relaxation time λ of the generalized Maxwell

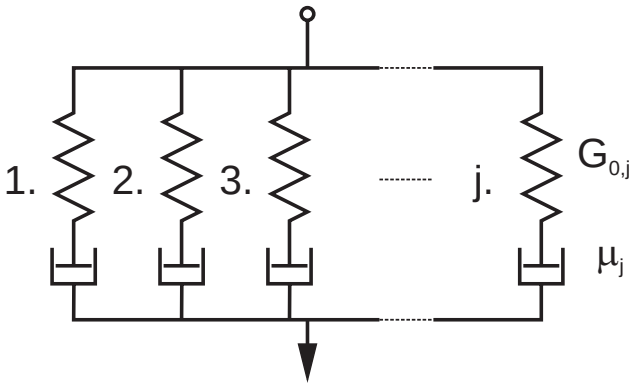

Figure 3: generalized Maxwell model

model equation 8 can be used. This equation contains the zero-shear-rate-viscosity μ_0, that describes the constant viscosity range for low shear rates. μ_0 is calculated with equation 9.

$$\lambda = \frac{1}{\mu_0} \cdot \sum_{j=1}^{z} G_j \cdot \lambda_j^2 \tag{8}$$

$$\mu_0 = \sum_{j=1}^{z} G_j \cdot \lambda_j \tag{9}$$

For a detailed description of the generalized Maxwell model please refer to <20; 23; 24>.

2.4. Estimation of fluid properties for the LVE-range

To define a certain generalized Maxwell model, several oscillation tests are necessary. With a frequency sweep, the parameters of the LVE-range can be analysed, especially the relaxation function respectively the relaxation time λ. The resulting parameters of a frequency sweep are valid for the LVE-range only. To ensure applicable measurements, a amplitude sweep is necessary to

identify the LVE-range limit, represented by a characteristic shear amplitude λ_{LVE}, before a frequency sweep is performed.

In the context of this paper, all generalized Maxwell models are developed according to a proposal by Baumgaertel and Winter <24>. This proposal estimates the spectrum of the relaxation function for all elements as well as their relaxation times and the quantity of the Maxwell elements.

3. Procedures to design an agitator

In this study, only the procedures by Metzner and Otto, which is based on the shaft speed, respectively the procedure by Reviol, which is based on the power of the agitator, will be considered. Both procedures will be shortly summarized in the following:

The shaft speed based concept by Metzner and Otto

Metzner and Otto investigated a Rushton turbine for laminar fluid flow. The limit of the laminar range was specified by $Re = 10$ <25; 26; 27>. Metzner and Otto postulated a proportionality between the agitator's shaft speed n and a representative shear rate $\dot{\gamma}$, see equation 10 <1>. The introduced proportional factor K_{MO} was identified being specific for the agitator's geometry.

$$\dot{\gamma} = K_{\mathrm{MO}} \cdot n \tag{10}$$

Although the concept of Metzner and Otto is criticised especially for its dependence on the mixed fluid, the concept became standard in dimensioning agitators <11; 19>.

The power based concept by Reviol

Reviol examined a propeller mixer in the laminar range too, but also for higher Reynolds numbers <7>. Coming from an analytic consideration of the agitator's power, Reviol identified a concept as shown in equation 11. Herein, Re is the Reynolds number, N_P the power number, while C_0 represents a factor, that is specific for geometry. Similar to K_MO, Reviol et. al. identified C_0 as being depend on the fluid <8; 9>. The shear rate $\dot{\gamma}$ is also a representative value for the entire agitator.

$$\dot{\gamma} \quad = \quad Re\, N_\mathrm{P} \cdot C_0 \cdot n \tag{11}$$

A special issue of the concept is its ability to be transformed into Metzner and Ottos concept for laminar fluid flow because of the constant character of the product of Reynolds number Re and power number N_P in this range, as described by Rushton <25; 26>.

The procedures described above are both based on a relationship between the agitator's shaft speed n and the representative shear rate $\dot{\gamma}$. For a design point related to the shaft speed n^* the representative viscosity μ^* can directly be calculated. With this value, a Reynolds number and also a power number can be derived, if the function $N_\mathrm{P} = f\,(Re)$ was examined before. From the power number N_P^* the needed power P^* can be derived. Figure 4 shows a scheme of the procedure, beginning with the shaft speed n^*. A more detailed description can exemplarily found in <10> and <28>.

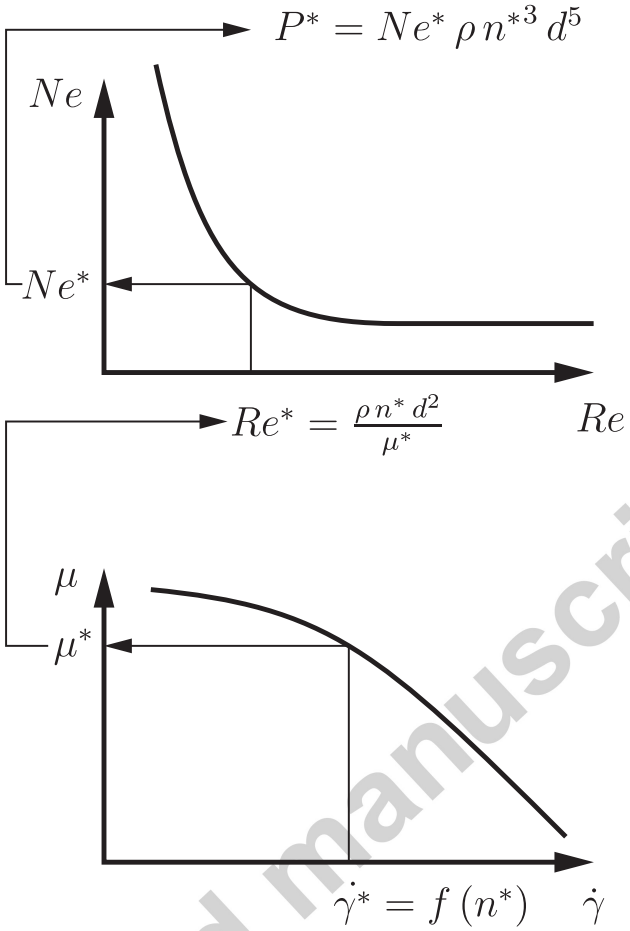

Figure 4: procedure of estimating the agitator's power, based on the shaft speed n^*

4. Investigated Fluids

For the estimation of the influence of fluid properties on the power consumption, these properties must be known at first. In this study the parameters to describe purely viscous fluids as well as the parameters to describe viscoelastic fluids had to be quantified. Concerning purely viscous properties, these parameters were measured by rotation viscometry. The viscometer was a searl-type viscometer by Brookfield. The viscoelastic properties of the fluid

were analysed by several oscillation tests. All oscillation tests were performed in a plate to plate arrangement with a viscometer from Haake.

4.1. Fluids with minor viscoelastic characteristics

The modelling of purely viscous fluid flow was achieved by three aqueous Carboxymethyl-Cellulose(CMC)-mixtures. The examined mixtures were built with the CMC-concentrations $c_1 = 1.0\ wt\%$, $c_2 = 1.5\ wt\%$ and $c_3 = 2.0\ wt\%$. The inserted CMC was of the type Walocel CRT 40000 PV by Dow. All mixtures were manufactured by mixing CMC-powder in water with a laboratory mixer. Before measuring the samples, all samples were subjected to a rest period of 24 hours.

In a first step, a rotation test was performed to estimate the shear viscosity of all three CMC-mixtures. Each mixture was measured at least five times. The results of all measurements are summarized by the functions of the shear viscosity over the shear rate, as can be seen in figure 5. The graph only shows the mean values of all measurements of each mixture. Figure 5 also discloses the standard deviation of each measurement point.

Especially for low shear rates, the standard deviation increases. In this range, flow reactive forces within the viscometer were too low for the limits of the intended measurement devices. For the following approximation with the power law according to equation 3, the range described above was neglected to avoid the influences of limited accuracy of the measurement device on the quality of the obtained parameters. The negligence of the range is also important due to the proximity to the zero-shear-rate-viscosity μ_0. In the range of the zero-shear-rate-viscosity, power laws are inadequate to represent the behaviour of the fluid. For each concentration, the mean values of all

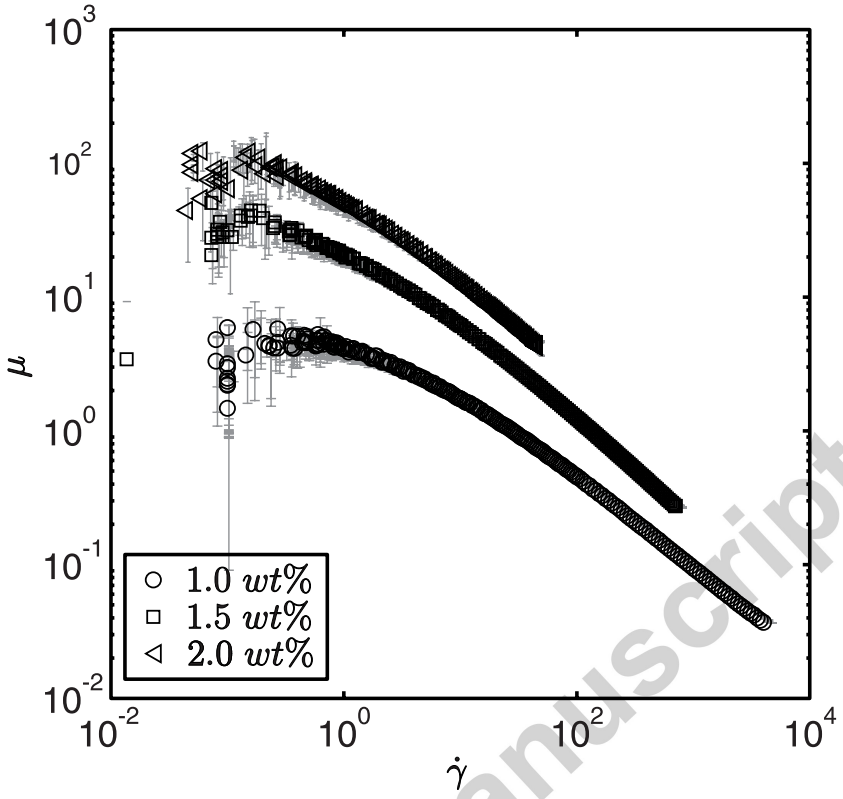

Figure 5: curves of viscosity for all investigated CMC-mixtures, mean values

estimated Parameters are summarized in tabular 1.

In the next step, the viscoelastic properties of the mixtures were investigated. For this, new samples of all mixtures were manufactured to obtain unstressed samples. This proceeding is necessary to avoid the influence of structural injuries as a result of the shear tests or ageing effects. The methodology of the experiments contains at least three series of measurements for all CMC-mixtures. In these series, several oscillation tests were performed and each were repeated at least five times for any series. Due to simplicity, the following presentations of viscoelastic properties only contain representative results from the first series of measurements.

Table 1: Parameters of the power law function for the three CMC-mixtures, mean values

$c\ [wt\ \%]$	$k\ [Pas^m]$	$m\ [-]$	$a\ [Pa\ \%]$
1.0	8.25	0.3949	3.808
1.5	41.13	0.2794	19.85
2.0	100.6	0.2346	50.47

To obtain the viscoelastic fluid parameters, several oscillation tests were performed, as mentioned before. At first, an amplitude sweep was carried out to identify the LVE-range. All amplitude tests were performed for a specified frequency. The frequency is from minor importance for the LVE-range limit and was chosen as $\omega = 10\ rad/s$ because of industrial practice <22>. The shear deformation was enlarged from $\gamma_0 = 0.01$ to $\gamma_0 = 10$. Subsequently, a frequency sweep has been performed. The limit for shear deformation was in each case chosen according to the estimated value of the amplitude sweep. The frequency ranged from $f = 0.01\ Hz$ to $f = 10\ Hz$. As a result of the frequency sweep, storage modulus G' and loss modulus G'' of all three CMC-mixtures were estimated. The course of these parameters can be seen in figure 6.

Based on the results of the frequency sweep, the relaxation functions $G(t)$ of all CMC-mixtures were calculated. Figure 7 illustrates the results. As can be seen, the results of each mixture are very similar.

The calculation of the generalized Maxwell model was performed according to the adaption by Baumgaertel and Winter <24>, so the quantity of the single Maxwell elements was estimated by a numerical procedure. Not less than four and at most six elements were applied.

The procedure of the generalized Maxwell model delivers the relaxation

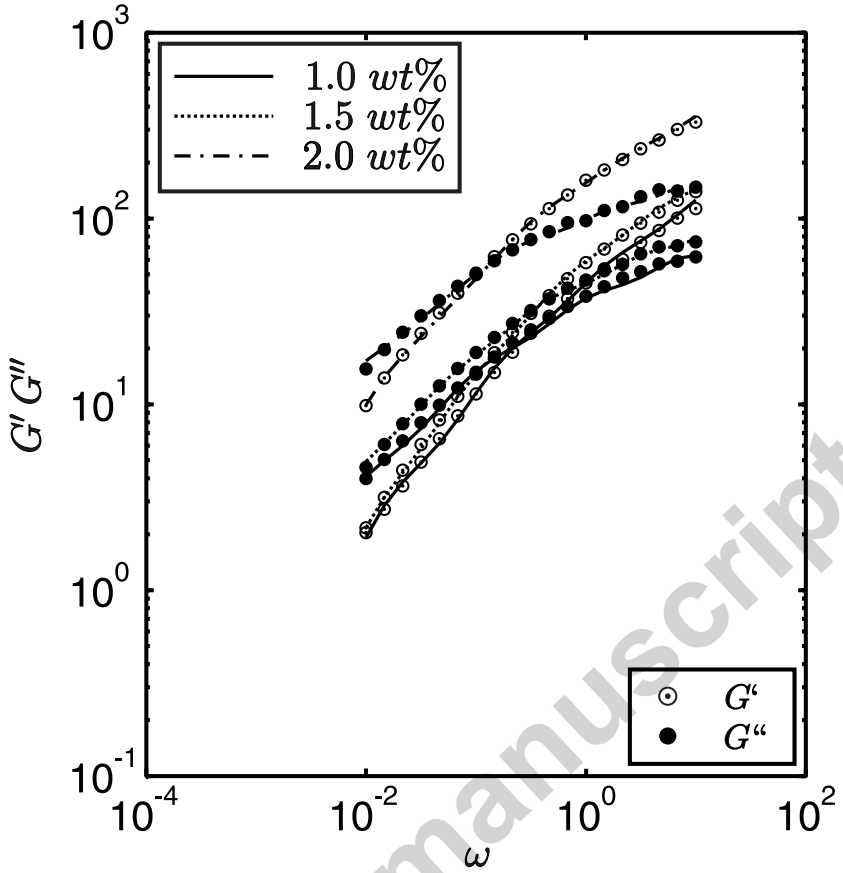

Figure 6: Storage- and loss modulus of the three CMC-mixtures, representative results from the first series of measurements

function as well as the relaxation time. The examined relaxation times and the before measured limits of each LVE-range are summarized in tabular 2. The relaxation time ranges from $\lambda = 55\ s$ to $\lambda = 75\ s$, so all relaxation times are close together, as could be assumed for similar relaxation functions. Hence, in the following a minor viscoelastic behaviour of CMC-mixtures will be assumed.

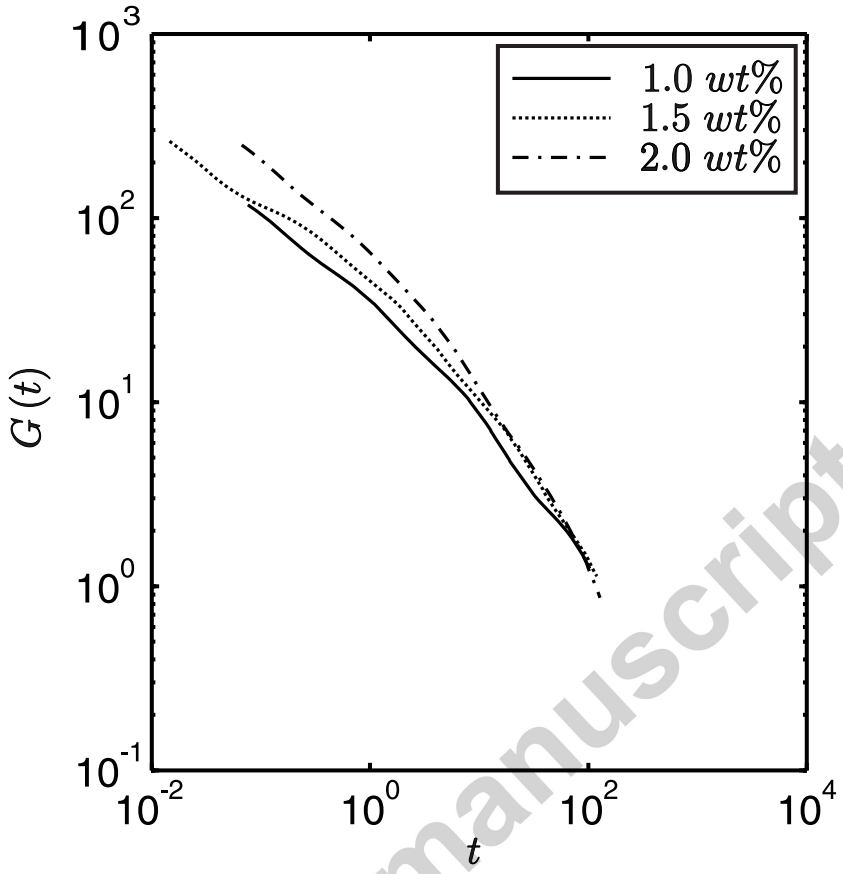

Figure 7: relaxation function of the three CMC-mixtures, representative results from the first series of measurements

4.2. Fluids with distinct viscoelastic characteristics

To obtain a fluid with distinct viscoelastic properties, three aqueous Polyacrylamide(PAA)-mixtures were created. The following three concentrations of the mixtures were chosen: $c_1 = 1.0\ wt\%$, $c_2 = 1.5\ wt\%$ and $c_3 = 2.0\ wt\%$. The mixtures were manufactured with PAA-granulate by Carl-Roth GmbH. The production process as well as the investigations to determine viscous and viscoelastic fluid properties of the mixtures were in the same way than for the CMC-mixtures.

Table 2: Parameters of the power law function for the three CMC-mixtures, mean values

$c\ [wt\ \%]$	$\gamma_{\mathrm{LVE}}\ [-]$	$\lambda\ [s]$
1.0	0.1924	54.93
1.5	0.1677	67.78
2.0	0.1498	73.51

Figure 8 illustrates the curves of viscosity for the three investigated PAA-mixtures. In the range of low shear rates, the measurement was less accurate due to the limited exactness of the measurement device, as already mentioned above. The range of low accuracy was neglected when applying equation 3 to obtain the fluid parameters. These are summed up in tabular 3.

Table 3: Parameters of the power law function for the three PAA-mixtures, mean values

$c\ [wt\ \%]$	$k\ [Pas^m]$	$m\ [-]$	$a\ [Pa\ \%]$
1.0	2.45	0.3282	1.070
1.5	7.16	0.2717	1.948
2.0	15.14	0.2364	3.968

As can be seen in tabular 1 and 3, the flow indices of all investigated fluids are in the same range for each concentration. A similar purely viscous behaviour of all analysed fluids can be certainly expected.

Furthermore, figure 8 shows an ascending slope for all viscous curves in the range of high shear rates. The crossover from the power-law range to the infinite-shear-rate viscosity μ_∞ was probably reached. For this range, power laws become void. In this paper, the approximation with equation 3 caused a very low error sum of squares, so the validity of equation 3 was still assumed.

All experiments to determine viscoelastic fluid properties were developed in the same way than for CMC-mixtures. Samples of all PAA-mixtures were

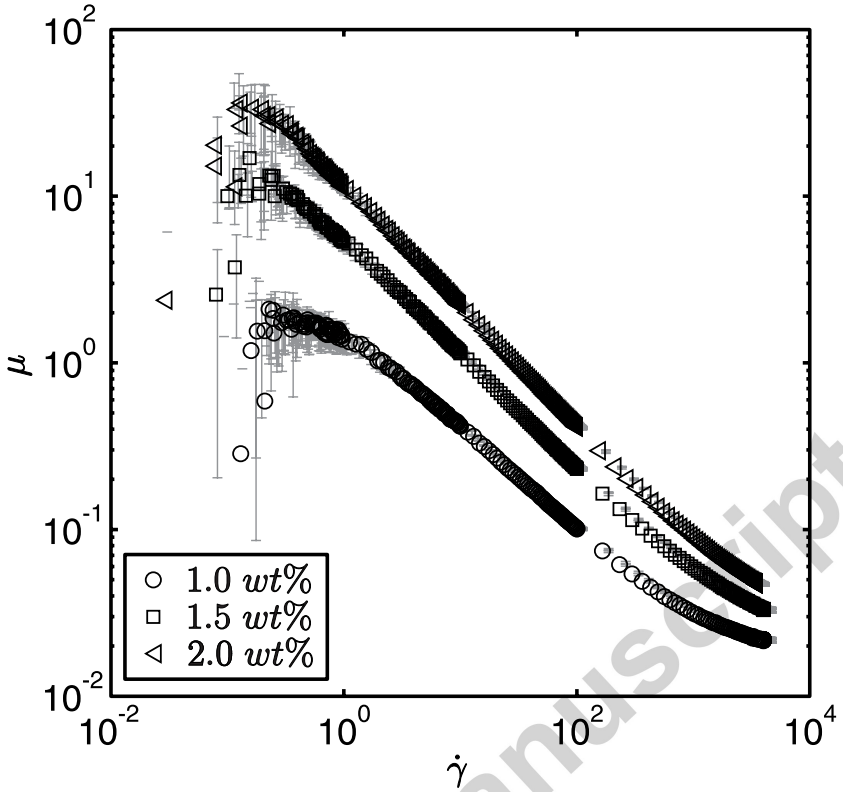

Figure 8: curves of viscosity for all investigated PAA-mixtures, mean values

newly manufactured to avoid damages as a reason of shear tests and ageing effects. At the beginning of the experiments, the limit of the LVE-range was identified by amplitude sweeps. In the following frequency sweeps, relaxation and loss modulus were determined. The number of repetitions of all experiments was just as for the experiments to investigate the CMC-mixtures.

From the frequency sweeps the storage modulus G' and loss modulus G'' are resulting. These are depicted in figure 9 for all PAA-mixtures. Based on both moduli, the relaxation function $G(t)$ of each PAA-mixture was calculated. The course of the resulting curves are presented in figure 10. A clear spacing between all mixtures can be identified.

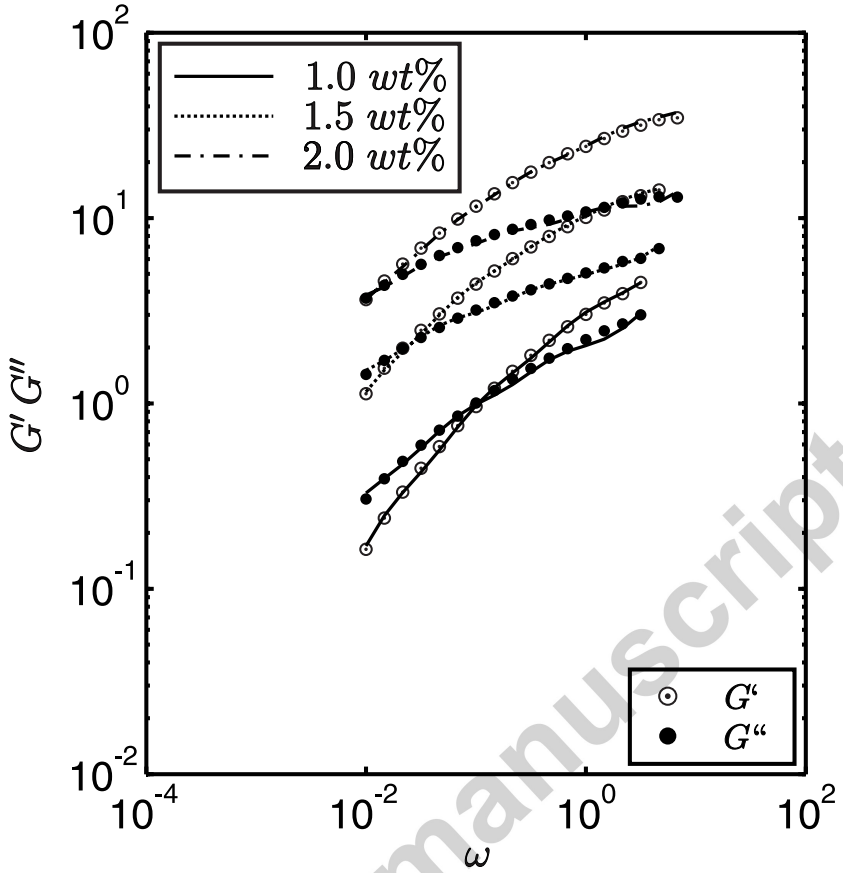

Figure 9: Storage- and loss modulus of the three PAA-mixtures, representative results from the first series of measurements

The procedure to determine the relaxation modules of the PAA-mixtures also requires an approximation by a generalized Maxwell model. In this study the adaption by Baumgaertel and Winter <24> leads to three up to five single Maxwell models.

The calculation of the relaxation function delivers also the relaxation time of each mixture. Corresponding to the space between each relaxation function, the characteristic time rises with increasing PAA-concentration from $\lambda = 49.09\ s$ to $\lambda = 117.8\ s$ in an strong manner. Because of the higher

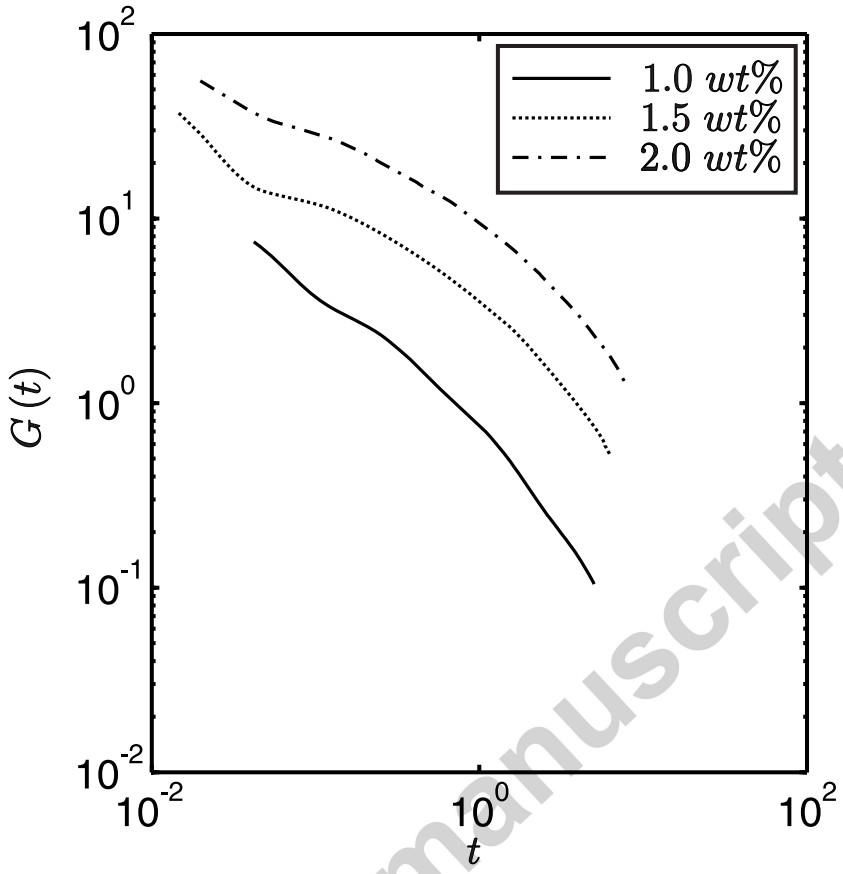

Figure 10: relaxation function of the three PAA-mixtures, representative results from the first series of measurements

values in comparison to the relaxation time of the CMC-mixtures, a definite distinct viscoelastic behaviour of PAA-mixtures will be supposed, especially due to the rising values within the different concentrations of PAA. The calculated relaxation times and the estimated limits of the LVE-range are summarized in tabular 4.

4.3. Comparison of all considered fluids

To compare the viscous behaviour of fluids, their viscosity curves can be considered and a clear impression is resulting. An also clear methodology to

Table 4: Parameters of the power law function for the three PAA-mixtures, mean values

$c\ [wt\ \%]$	$\gamma_{\mathrm{LVE}}\ [-]$	$\lambda\ [s]$
1.0	0.1932	48.46
1.5	0.1506	104.51
2.0	0.1564	117.92

compare viscoelastic fluid properties was introduced by Pipkin <29>. Pipkin proposed the plot of a characteristic shear amplitude, e.g. the limit of the LVE-range, over Deborah's number. In the present paper, the Deborah number was calculated according to equation 12. Herein, ω is the characteristic rotary frequency, as chosen for the amplitude sweeps and refers to a value of $\omega = 10\ rad/s$.

$$De = \omega \cdot \lambda \tag{12}$$

In figure 11, Pipkin's diagram for the considered fluids is shown. All figures above, containing viscoelastic fluid properties, only contained selected results due to a simple illustration. In this final results, the measurement values of all experiments were taken into account. So the deviations of all measurements are depicted too.

As can be seen, all CMC-mixtures are characterized by lower Deborah numbers than PAA. Especially the concentration $c_2 = 1.5\ wt\%$ and $c_3 = 2.0\ wt\%$ are close together. The PAA-mixtures causes higher Deborah numbers. Only the sample with $c = 1.0\ wt\%$-PAA is characterized by a lower Deborah number, than two CMC-mixtures. Remarkable is the big step size between the single PAA-mixtures. The limit of the LVE-range is in the same order for all considered fluids.

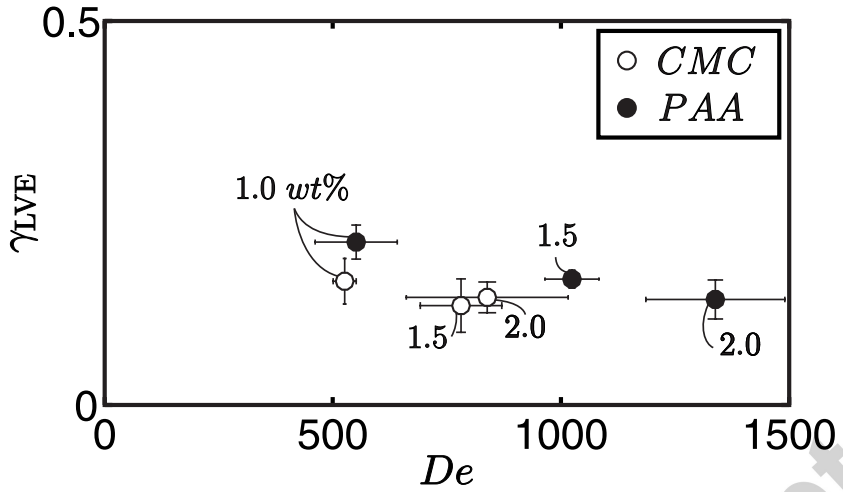

Figure 11: Pipkin's Diagram for the CMC- and PAA-mixtures, mean values of all series of measurements

5. Experimental setup

The test bench is illustrated in figure 12, containing the agitator device and the circular vessel. For visual observation, the vessel was manufactured in Polymethylmethacrylate. The diameter of the vessel amounts 290 mm and the height 492 mm. The resulting volume is about 32.5 l.

On the top of the vessel, the agitator device can be connected coaxially. The agitator is a propeller mixer (1), which is engaged to a DC motor (2). Between agitator and motor, a sensor (3) is placed to record torque and shaft speed. The measurement range of the sensor reaches from up to 0.5 Nm for torque. The motor can be regulated by a control unit. The maximum shaft speed is continuously adjustable and amounts 200 min^{-1}. An additional sensor observes the fluid temperature near the agitator. The applied sensor is of the type PT100.

The final analysis of the measurement values will be performed by a

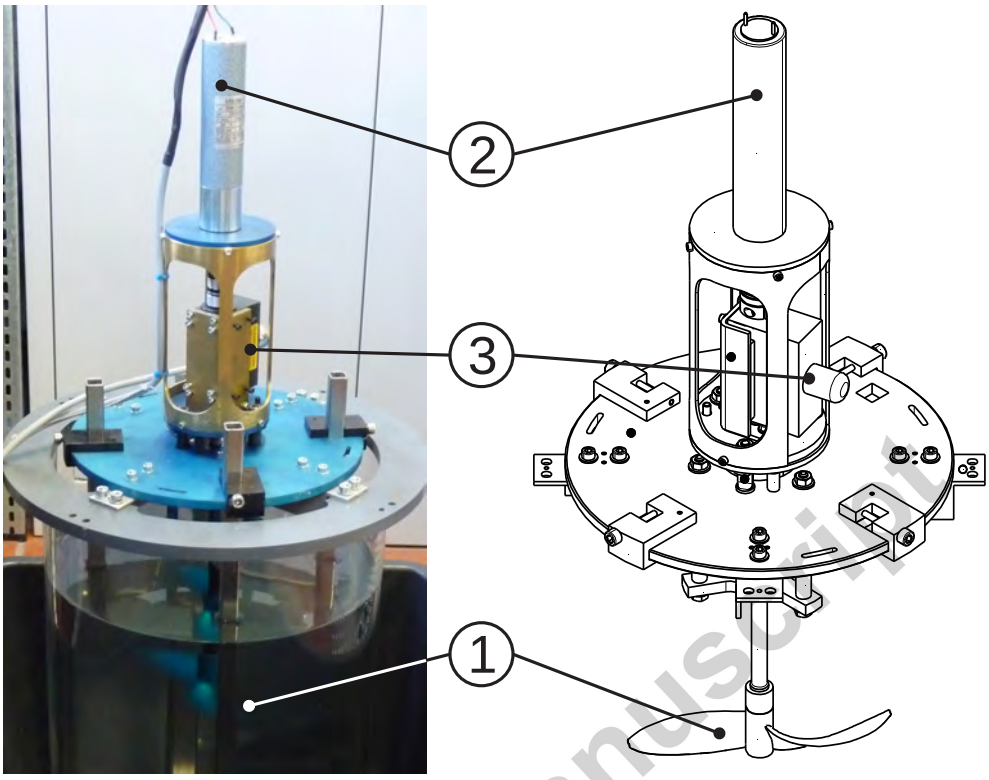

Figure 12: Test bench

matlab-based algorithm and contains sub-algorithms to execute the different design procedures as described in chapter 3.

6. Experimental results

As shown in chapter 3, the power consumption for agitating non-Newtonian fluid flow will be estimated indirectly with the function $N_{\mathrm{P}} = f\,(Re)$, see also figure 4. This means, a specific design point P^*, which is based on N_{P}^* must be calculated by the function composition $Re^* \circ \mu^*$. The effective shear viscosity μ^* is calculated by the power law according to equation 3 and with a design procedure referred to equation 10 or 11. Both design procedures

include a proportionality factor that is depending on the mixed fluid. Hence, the influence of the fluid properties will be best represented by the proportionality factors. For this, the presentation of the experimental results will be done by depicting the proportional factors instead of the estimated power curves.

The experiments that are the basis of the following presented proportionality factors were repeated at least five times. To evaluate the parameters, first all experimental data was averaged. The depicted error bars result from using the standard deviation. The approximation of the power-law range of the fluid was performed according to equation 3. The usage of Ostwald's and DeWaele's power law, see equation 2, was sufficient too, but the estimated error sum squares were higher than for equation 3.

6.1. Fluids with minor viscoelastic characteristics

Figure 13 shows the course of the proportionality factor K_{MO} which was introduced by Metzner and Otto. Instead of its definition, the factor was treated as a function of the Reynolds number. So the value of K_{MO} was repetitively calculated for each measured Reynolds number. Notice the character of the Reynolds number as an effective number. Figure 13 contains the results of all three CMC-mixtures.

The distribution of the measurement values shows a monotonically increasing trend. An exception can be found as a local extremum for all mixtures. Furthermore, a clear distinction of all mixtures can be identified. The measurement faults in case of low Reynolds numbers are caused by small reactive forces for small shaft speed and the limit of the applied sensors. However, the large measurement error of the measurements with a

concentration of $c_3 = 2.0\ wt\%$ are not resulting from reactive forces. As a conditional of manufacturing the samples, air was dispersed. Probably, the dispersed air causes highly differing values in torque, but the trend was estimated plausible, as the comparison with the results of the other mixtures substantiate. The experiments with lower concentration were not concerned.

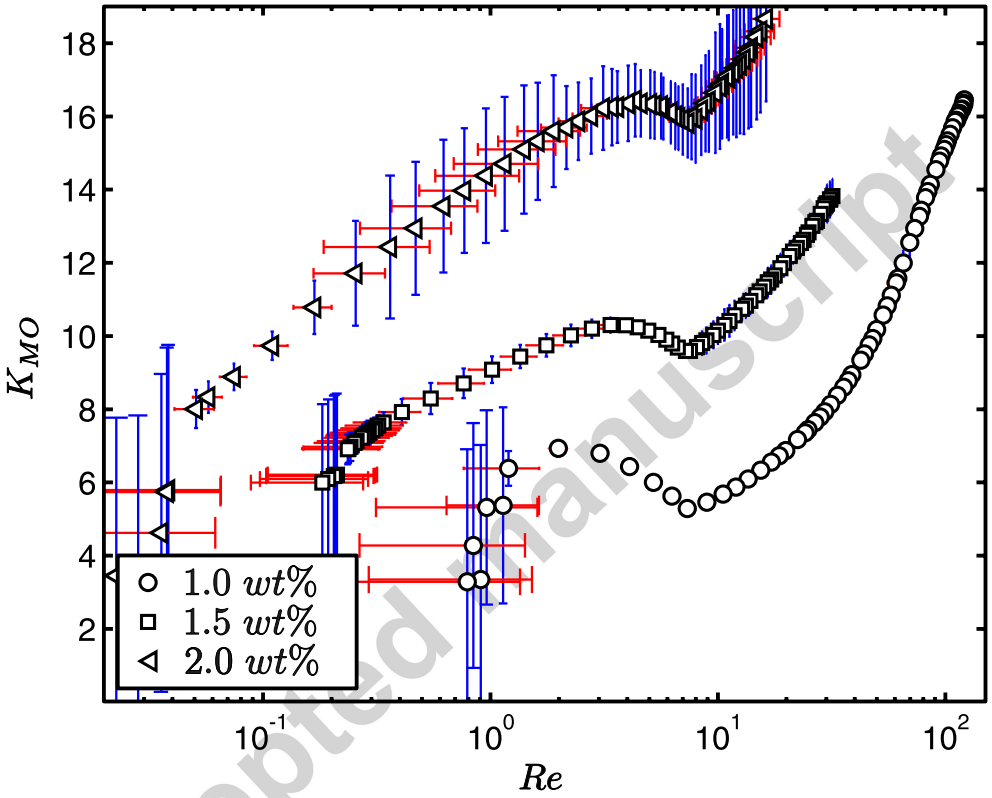

Figure 13: Course of K_{MO} as a function of Re, results for all CMC-mixtures, represented by mean values

Figure 14 illustrates the course of the proportionality factor C_0 as a function of the effective Reynolds number. All investigated concentrations are presented. The data for C_0 are also at first rising and differing for varying concentrations, as seen before in figure 13 for K_{MO}. It has to be mentioned,

that next to this range a plateau-like course is following, which is characterized by nearly constant values.

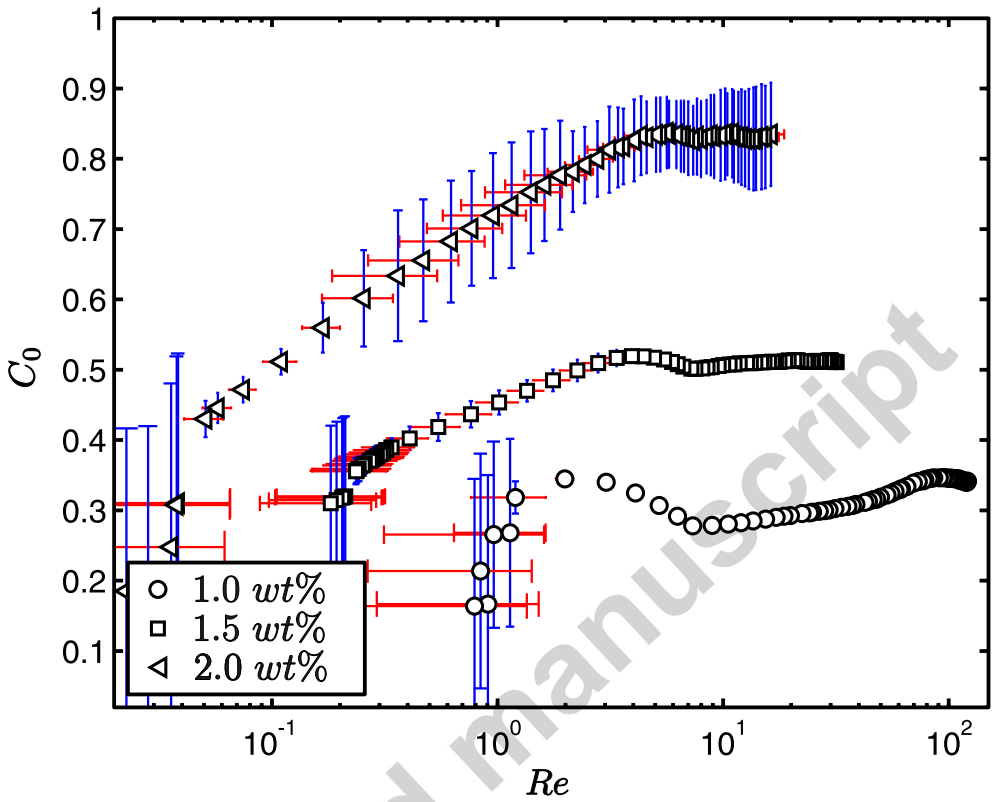

Figure 14: Course of K_{MO} as a function of Re, results for all CMC-mixtures, represented by mean values

The extrema, shown in figure 13, and the starting point of the depicted plateau ranges in figure 14, can both be localized at Reynolds numbers of about $Re \approx 10$.

6.2. Fluids with distinct viscoelastic characteristics

All measurements, performed in PAA-mixtures that are analysed under the terms of Metzner's and Otto's concept, are summarized in figure 15.

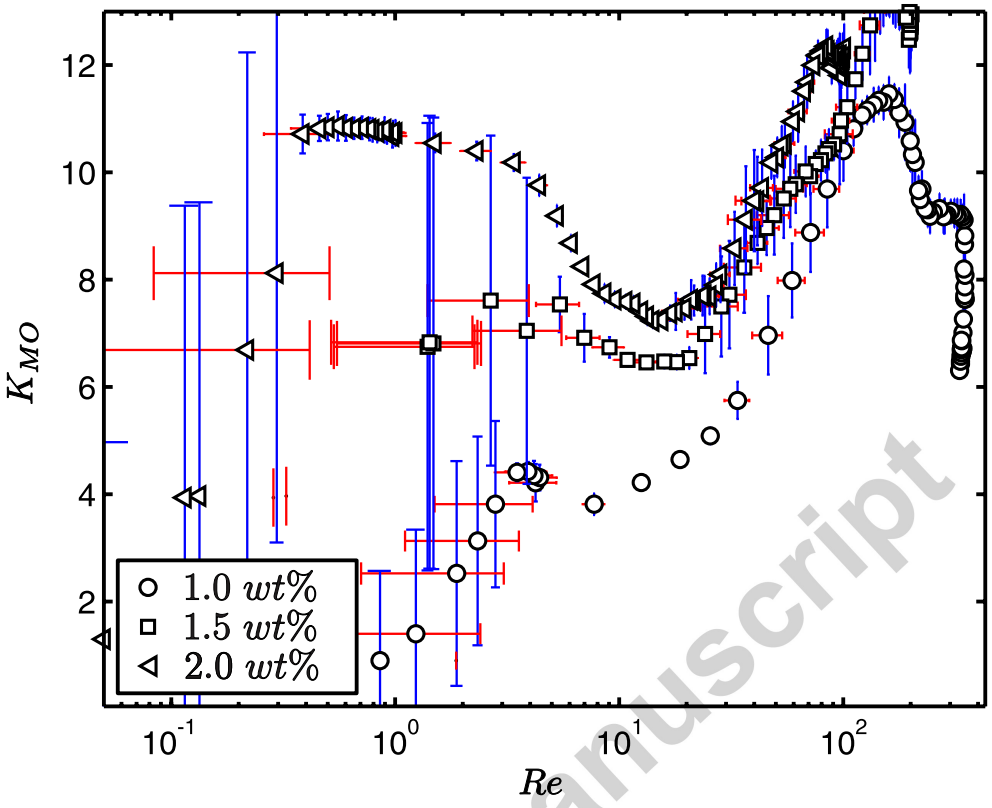

Figure 15: Course of K_{MO} as a function of Re, results for all PAA-mixtures, represented by mean values

The plot shows first rising then decreasing and in the following again rising values in the range of low Reynolds numbers from about $Re \approx 0.1$ to approximately $Re \gtrsim 10$. For higher Reynolds numbers of about $Re \gtrsim 100$ the values are decreasing again but this time in a strong manner. The results also show the variation of the proportionality factor for the differing concentrations of PAA, as seen before in figure 13 and 14. But as can be seen for PAA, the spacing between the curves is lower than for CMC.

The reason for measurement faults in the range of low Reynolds numbers are also coming along with the small reactive forces for small shaft speeds.

So, the limited measurement range of the sensors will cause the in figure 15 shown deviations.

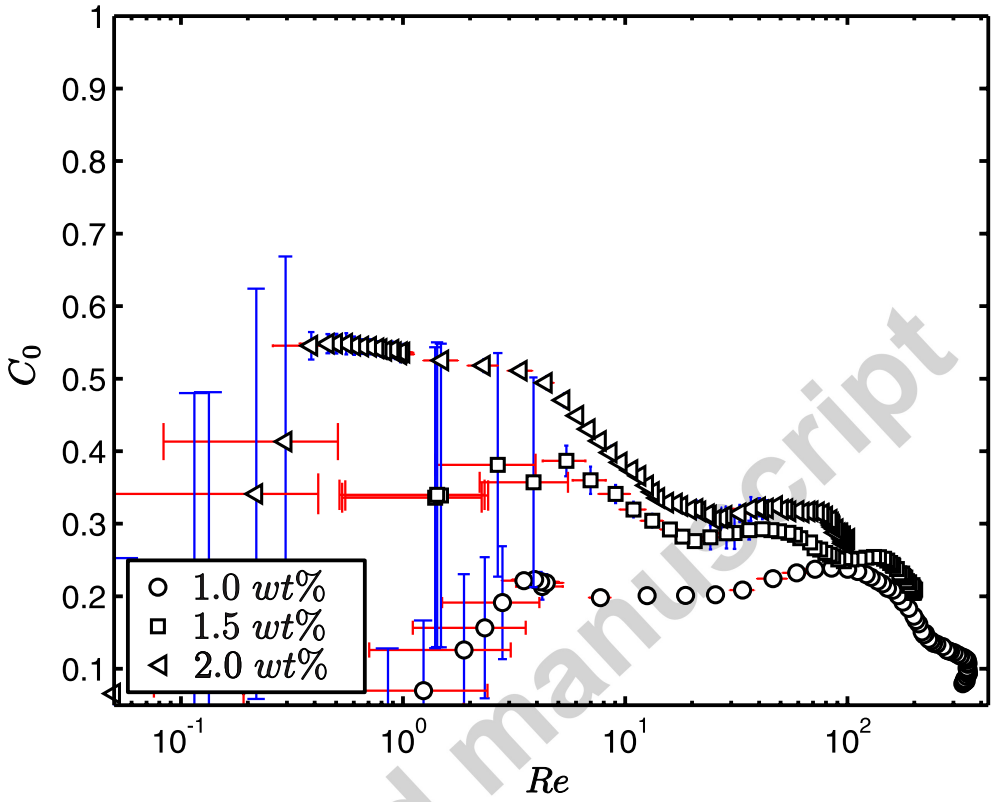

Figure 16: Course of C_0 as a function of Re, results for all PAA-mixtures, represented by mean values

The course of the proportionality factor C_0 is illustrated in figure 16. The plot contains all with PAA performed experiments and shows a similar magnitude order as seen before in figure 14 for CMC. Comparing the for PAA-mixtures obtained proportionality factors of both concepts with each other, it is evident that C_0 shows a smoother trend, although a constant range is not prevalent too. Except for a small scope in case of low Reynolds numbers, the trend of the course is monotonically decreasing with a clearly

rising slope for increasing Reynolds numbers.

7. Discussion

The results presented in figure 13 till 16 show two different kinds of dependencies. On the one hand, the proportionality factors are depending on the flow characteristics, represented by the Reynolds number. On the other hand, the factors were influenced by the fluid itself as already has been mentioned in the introduction of this study.

Both influences will now be discussed, starting with the factor's dependency on the Reynolds number:

Reynolds dependencies

The investigations of fluids with minor viscoelastic character (CMC) disclose the presence of a plateau range for the proportionality factor C_0 in the scope of high Reynolds numbers. Before the plateau range is reached, curves are characterised by a rising trend. The plateau itself is always reached for Reynolds numbers of about $Re \approx 10$. Because of the high measurement faults for low Reynolds numbers, the influences on the rising trend can't be clearly identified. But it is remarkable, that the change happens in the laminar flow regime. Be aware, that the definition of the region as laminar has been proposed by Rushton <25>. The flow characteristic was not proven in this study. In contrast with the shaft speed based concept by Metzner and Otto, which leads to variable values for the whole measured range, the power based concept by Reviol is more adequate for fluids with minor viscoelastic character, here represented by aqueous CMC-mixtures.

The investigations performed with fluids disposing distinct viscoelastic characteristics (PAA) bared the unreliability of the shaft speed based concept by Metzner and Otto. The herein introduced proportionality factor changes many times for increasing Reynolds numbers and therefore a strong dependency can be presumed. The proportionality factor, introduced by Reviol, is also a variable for viscoelastic fluid flow, but the trend of the course is consistently in sections. Overall, the trend is monotonically decreasing. In both concepts, a small scope with a strong increasing slope and the range of high measurement faults can be found for low Reynolds numbers. Hence, the influence of the increasing slope can't be clearly identified. The sudden decline of the courses for high Reynolds numbers are also remarkable. Especially for Metzner's and Otto' concept, the decline can be seen obviously, but also Reviol's concept discloses a decline for this range. Possibly, this decline is caused by the inadequate approximation of the PAA-mixture's viscosity curves by a power law. In chapter 4, the proximity to the range of infinite-shear-rate-viscosity μ_∞ for all PAA-mixtures was already mentioned as well as the disability of power laws to describe non-power law regions, see chapter 2.1. This indicates the necessarity of more complex models to approximate the viscosity curves.

Fluid dependencies

In addition to the dependencies on the Reynolds number, the investigations examined an influence of both concepts on the fluid properties. With increasing concentrations of CMC respectively PAA, the proportional factors of the considered concepts were changing. This indicates the imperative to extend the considered concepts, when applying them on viscoelastic fluid

flow. Several researchers already proposed modifications for the proportionality factor of Metzner's and Otto's concept: Calderbank and Moo-Young as well as Rieger and Novak pointed out the significance of the flow index m, on the power law according to equation 2 <3; 30>. Refer e.g. to <31> for further informations. Reviol also discovered the influence of the proportional factor on his concept. He considered this influence by the consistency k of the approximation by Ostwald's and DeWaele's power law.

Reviol exposed in his examinations, that the shaft speed based concept by Metzner and Otto is a special case of the power based concept <7>. Hence, in the following only the power based concept will be discussed because of the imperative relevance for both concepts:

Some of the influences described above, can be connected with the usage of an effective shear rate for the agitator to represent the total kinematics of a design point. Reviol discovered in the derivation of his concept the need of an apparent viscosity to correlate shaft speed and shear rate, instead of the more accurate viscosity function. The apparent viscosity is assumed as beeing characteristic for the whole process. Furthermore, this characteristic viscosity is used to calculate an effective Reynolds number and this number will finally lead to a power number based on a power characteristic that was achieved by Newtonian fluid flow before. The last step presumes a correlation between Newtonian and non-Newtonian fluid flow that is not given as can be shown by dimensional analysis. In addition the derivation of the concept neglects the influence of normal stress components and stress relaxation effects. Hence, the description of viscoelastic fluid properties is not provided by this concept

<7>.

The identification of the inadequate modelling of the fluid properties in the fundamentals of the concepts as the reason for dependencies on fluid flow is in good accordance to the results of the power based concept. Hence the power based concept is only valid for fluids with minor viscoelastic behaviour. To include viscoelastic fluid properties the extension of the considered concepts is necessary.

8. Summary

In the present paper, the influence of viscoelastic fluid properties on the power consumption of mixing processes was investigated. For this, the well-known shaft speed based concept by Metzner and Otto and the power based concept by Reviol was chosen.

To identify the influence of viscoelastic behaviour, fluids with different distinct viscoelastic properties were adopted. For the approximation of nearly purely viscous fluids, aqueous Carboxymethylcellulose-(CMC)-mixtures were intended. However, the performed investigations showed a minor viscoelastic characteristic. Fluids with a distinct viscoelastic characteristic were represented by aqueous Polyacryl-amide-(PAA)-mixtures.

The determined results show a clear influence of the fluid characteristics on the used concept which will directly influence the design of the mixer. Furthermore, it is clearly shown, that purely viscous fluid properties affect the design process in another way, than viscoelastic fluid properties. One reason for this can be found in the inadequate consideration of viscoelastic fluid properties in the fundamentals of the investigated concepts.

Symbols

a	$[Pa]$	Curve parameter
c	$[wt\%]$	Concentration in percent by weight
C_0	$[-]$	Proportionality factor
d	$[m]$	Diameter
$De = \omega\lambda$	$[-]$	Deborah number
f	$[Hz]$	Frequency
$G_0 = G(0)$	$[Pa]$	Rigidity modulus
$G(t)$	$[Pa]$	Relaxation function
G'	$[Pa]$	Storage modulus
G''	$[Pa]$	Loss modulus
j	$[-]$	Counter variable
K_{MO}	$[-]$	Proportionality factor
k	$[Pas^m]$	Consistency
m	$[-]$	Flow index
n	$[s^{-1}]$	Shaft speed
$N_{\mathrm{P}} = \frac{P}{\rho n^3 d^5}$	$[-]$	Power number
P	$[W]$	Power
$Re = \frac{\rho n d^3}{\mu}$	$[-]$	Reynolds number
t	$[s]$	Time
z	$[-]$	Quantity of Maxwell elements

Greek Symbols

Literature

[1] A. B. Metzner, R. E. Otto, Agitation of non-newtonian fluids, AlChE J. 3 (1) (1957) 3–10. doi:10.1002/aic.690030103.

[2] F. Rieger, V. Novak, Scale-up method for power consumption of agitators in the creeping flow regime, Chem. Eng. Sci. 27 (1) (1972) 39–44. doi:10.1016/0009-2509(72)80139-8.

γ_0	$[-]$	Shear strain
γ_{LVE}	$[-]$	LVE-range limit
$\dot{\gamma}$	$[s^{-1}]$	Shear rate
λ	$[s]$	Relaxation time
μ	$[Pas]$	Shear viscosity
μ_0	$[Pas]$	Zero-shear-rate-viscosity
μ_∞	$[Pas]$	Infinite-shear-rate-viscosity
ρ	$[kg/m^3]$	Density
τ	$[Pa]$	Shear stress
ω	$[s^{-1}]$	Frequency

[3] F. Rieger, V. Novak, Power consumption of agitators in highly viscous non-newtonian liquids, Trans. Inst. Chem. Eng. 51 (1973) 105–111.

[4] F. Rieger, V. Novak, Power consumption scale-up in agitating non-newtonian fluids, Chem. Eng. Sci. 29 (11) (1974) 2229–2234. doi:10.1016/0009-2509(74)80031-X.

[5] H. Henzler, G. Obernosterer, Effect of mixing behaviour on gas-liquid mass transfer in highly viscous, stirred non-newtonian liquids, Chem. Eng. Technol. 14 (1991) 1–10. doi:10.1002/ceat.270140102.

[6] K. H. Wassmer, H. K. D., A unified model for the mixing of non-newtonian fluidsin the laminar, transition, and turbulent region, Macromol. Mater. Eng. 290 (4) (2005) 294–301. doi:10.1002/mame.200400328.

[7] T. Reviol, Experimentelle und numerische untersuchungen eines modifizierten propeller-viskosimeters zur bestimmung der fließeigenschaften nicht-newtonscher medien mit inhomogenem charakter, Dissertation, TU Kaiserslautern, Kaiserslautern (2010).

[8] T. Reviol, M. Böhle, Beitrag zur auslegungsprozedur von rührwerken

529 und anwendung an einem propellerviskosimeter, in: Vortragssammel-
530 band zum 16. Köthener Rührerkolloquium, Köthen, 2013, pp. 14–25,
531 ISBN:978–3–86011–067–6.

532 [9] T. Reviol, S. Kluck, M. Böhle, Erweiterung der auslegungsverfahren
533 von rührern und anwendung an einem propellerviskosimeter, Chem. Ing.
534 Tech. 86 (8) (2014) 1230–1240. doi:10.1002/cite.201300100.

535 [10] M. Kraume, Mischen und Rühren - Grundlagen und moderne Verfahren,
536 Wiley-VCH, Weinheim, 2003.

537 [11] H.-J. Henzler, Auslegung von Rührfermentern - Berücksichtigung der
538 nicht-Newtonschen Eigenschaften von Fermentationslösungen, Chem.
539 Ing. Tech. 79 (7) (2007) 951–965. doi:10.1002/cite.200600112.

540 [12] J. Ulbrecht, K. Wichterle, Schnell laufende Rührwerke bei lam-
541 inarer Strömung, Chem. Ing. Tech. 39 (11) (1967) 656–658.
542 doi:10.1002/cite.330391104.

543 [13] H. Höcker, G. Langer, U. Werner, Der leistungsbedarf von rührern in
544 nicht-newtonschen flüssigkeiten, Chem. Ing. Tech. 52 (11) (1980) 916–
545 917. doi:10.1002/cite.330521118.

546 [14] P. A. Tanguy, F. Thibault, E. B. de la Fuente, A new investigation of
547 the metzner-otto concept for anchor mixing impellers, Can. J. Chem.
548 Eng. 74 (2) (1996) 222–228. doi:10.1002/cjce.5450740207.

549 [15] J. Pawlowski, Prozessbeziehungen bei nicht newtonschen Stoffen - Kritik
550 des Metzner-Otto-Konzeptes, Chem. Ing. Tech. 76 (7) (2004) 910–914.
551 doi:10.1002/cite.200403388.

[16] G. Böhme, Consistent scale-up procedure for the power consumption in agitated non-newtonian fluids, Chem. Eng. Technol. 11 (1) (1988) 199–205. doi:10.1002/ceat.270110127.

[17] J. Kelkar, R. Mashelkar, J. Ulbrecht, On the rotational viscoelastic flows around simple bodies and agitators, Trans. Inst. Chem. Eng. 50 (1972) 343–352.

[18] J. V. Kelkar, R. A. Mashelkar, J. Ulbrecht, Scale-up method for the power consumption of agitators in the creeping flow regime, Chem. Eng. Sci. 28 (2) (1973) 664–668. doi:10.1016/0009-2509(73)80071-5.

[19] K. Wichterle, J. Proscaronkova, J. Ulbrecht, Schnell laufende Rührwerke bei laminarer Strömung. Teil II: Simulation des mechanischen Rührens durch einen rotierenden niedrigen Zylinder, Chem. Ing. Tech. 43 (15) (1971) 867–870. doi:10.1002/cite.330431506.

[20] G. Böhme, Strömungmechanik nicht-Newtonscher Fluide, 2nd Edition, Teubner, Stuttgart, 2000.

[21] R. Tanner, Engineering rheology, Oxford University Press, 2000.

[22] T. Mezger, Das Rheologie Handbuch, Vincentz Network, 2006.

[23] N. Phan-Thien, Understanding Viscoelasticity: Basics of Rheology, Springer, 2002.

[24] M. Baumgaertel, H. H. Winter, Determination of discrete relaxation an retardationt time spectra from dynamic mechanical data, Rheol. Acta 28 (6) (1989) 511–519.

[25] J. Rushton, E. Costich, H. Everett, Power characteristics of mixing impellers - part i, Chem. Eng. Prog. 46 (8) (1950) 395–404.

[26] J. Rushton, E. Costich, H. Everett, Power characteristics of mixing impellers - part ii, Chem. Eng. Prog. 46 (9) (1950) 467–476.

[27] M. Zlokarnik, Rührtechnik - Theorie und Praxis, Springer, Berlin, 1999.

[28] Handbuch der Rührtechnik, EKATO Rühr- und Mischtechnik GmbH, 1990.

[29] A. C. Pipkin, Lectures on Viscoelasticity, Springer, 1972.

[30] P. Calderbank, M. Moo-Young, The power characteristics of agitators for the mixing of newtonian and non-newtonian fluids, Trans. Inst. Chem. Eng. 39 (1961) 337–347.

[31] S. M. Shekar, S. Jayanti, Mixing of power-law fluids using anchors: Metzner-otto concept revisited, AlChE J. 49 (1) (2003) 30–40. doi:10.1002/aic.690490105.